

Indirect nonlinear interaction between toroidal Alfvén eigenmode and ion temperature gradient mode mediated by zonal structures

Qian Fang,¹ Guangyu Wei,¹ Ningfei Chen,¹ Liu Chen,^{1,2} Fulvio Zonca,^{2,1} and Zhiyong Qiu^{3,2}

¹*Institute for Fusion Theory and Simulation and Department of Physics, Zhejiang University, Hangzhou 310027, China*

²*Center for Nonlinear Plasma Science and C.R. ENEA Frascati, Via E. Fermi 45, 00044 Frascati, Italy*

³*Key Laboratory of Frontier Physics in Controlled Nuclear Fusion and Institute of Plasma Physics, Chinese Academy of Sciences, Hefei 230031, China*

(*Electronic mail: zqiu@ipp.ac.cn)

(Dated: 29 August 2024)

The indirect nonlinear interactions between toroidal Alfvén eigenmode (TAE) and ion temperature gradient mode (ITG) are investigated using nonlinear gyrokinetic theory and ballooning mode formalism. More specifically, the local nonlinear ITG mode equation is derived adopting the fluid-ion approximation, with the contributions of zonal field structure and phase space zonal structure beat-driven by finite amplitude TAE accounted for on the same footing. The obtained nonlinear ITG mode equation is solved both analytically and numerically, and it is found that, the zonal structure beat-driven by TAE has only weakly destabilizing effects on ITG, contrary to usual speculations and existing numerical results.

I. INTRODUCTION

Drift wave (DW) turbulence¹ and shear Alfvén wave (SAW)²⁻⁷ are two major categories of collective oscillations contributing to anomalous cross-field transport in magnetized plasmas. DWs are typically micro-scale electrostatic oscillations driven by free energy associated with thermal plasma density and/or temperature nonuniformities, and are widely accepted as candidates for inducing bulk plasma transport. On the other hand, SAW instabilities or, more precisely, Alfvén eigenmodes (AEs) due to equilibrium magnetic geometry excited by energetic particles (EPs), are expected to play crucial role in EP transport. DW and SAW instabilities are characterized by different spatiotemporal scales, driven unstable by different free energy sources and dominate transport of different energy regime, and, thus, are typically studied separately. However, it is expected that there are complex cross-scale couplings among DWs and SAWs in burning plasmas, due to the mediation by EPs^{7,8}. Specifically, on the one hand, EPs drive meso-scale SAW instabilities that can provide nonlinear feedback to both the macroscopic plasma profiles and microscopic fluctuations. On the other hand, EPs can linearly and nonlinearly (via SAWs) excite zonal structures (ZS)⁹⁻¹¹, thus act as generators of nonlinear equilibrium^{12,13}. There are now raising interest in their mutual effects on each other, due to the recent observed thermal plasma confinement improvement in the presence of EPs^{14,15}. E.g., experiments and simulations have indicated that the presence of EPs can significantly suppress ion temperature gradient (ITG) turbulence, thereby reducing ion thermal stiffness and enhancing ion confinement¹⁵. Early linear gyrokinetic simulations suggested that the presence of EPs might trigger internal transport barriers¹⁶ (ITBs) formation, which could decrease core turbulence levels and improve bulk plasma confinement.

There are several channels for linear stabilization of micro-turbulence by EPs via, dilution of destabilizing bulk ions¹⁷, EP-pressure induced Shafranov shift stabilization¹⁸, resonant

stabilization^{19,20}, electromagnetic stabilization^{16,21}, and so on. The linear stabilization effects are now relatively well understood, and interested readers may refer to a recent review for a more complete picture²².

Moreover, numerical studies have revealed a nonlinear mechanism for fast-ion-enhanced EM-stabilization of ITG²³, which could be much more stabilizing than linear ones²⁰, then these nonlinear coupling mechanisms have drawn significant research interest²⁴. A potential physical interpretation is that the presence of EPs provides marginally linearly stable EM-modes, i.e., toroidal Alfvén eigenmodes (TAEs)²⁵ that transfer energy nonlinearly to ZS^{26,27}, and the increase in ZS levels stabilizes the ion-scale turbulence^{24,28}. However, the underlying physical processes of this issue remain to be explored.

More recently, the direct nonlinear interactions among TAE and electron drift wave (eDW) are proposed and analyzed. It is found that direct nonlinear scattering by ambient eDWs may significantly reduce or even completely suppress TAE stability, due to radiative damping of the nonlinearly generated high- n KAW quasi-modes²⁹. On the other hand, for typical reactor parameters and fluctuation intensity, the “inverse” process, i.e., the direct nonlinear scatterings of eDW by ambient TAEs, have negligible net effects on the eDW stability³⁰, which differs from the results of previous simulations. To understand the bulk plasma confinement in the presence of EPs, as a natural step forward, in this work, we will investigate the in-direct nonlinear interaction among TAE and DWs mediated by ZS, i.e., the “linear” stability of DWs in the presence of ZS nonlinearly excited by TAE³¹.

ZS, including zonal flows (ZF), zonal currents (ZC), and more generally, phase space zonal structures (PSZS)^{12,32}, are known to play important roles in regulating micro-scale DW type instabilities including drift Alfvén waves (DAWs)^{31,33,34}. The regulation is achieved via the nonlinear generation of ZS by DWs/DAWs, and in the process, ZS scatters DWs/DAWs into linearly stable short radial wavelength domain. The ZS excitation can be achieved via the spontaneous excitation

via radial envelope modulation of DWs/DAWs^{31,33}, as well as beat-driven process of DW/DAW self-coupling frequently observed in large scale simulations, characterized by a ZF growth rate being twice of DW/DAW instantaneous growth rate^{35,36}. To simplify the analysis while focusing on the main physics picture of nonlinearly generated ZS on DW stability, in this work, we consider only the beat-driven process by TAE^{37,38}, without including the spontaneous excitation process. It is already shown analytically and numerically that, zero frequency radial electric field can significantly stabilize ITG via modification of the “potential well” depth³⁹. Here, using ITG as the paradigmatic model and following the analysis of Ref. 39, we will investigate the indirect nonlinear interaction between TAE and DW, mediated by ZS. Technically, this is achieved by deriving the expression of TAE beat-driven ZS, and taking it as a “nonlinear” equilibrium into the ITG eigenmode equation. Thereafter, the local dispersion relation and mode structure of the ITG under the influence of ZS are derived in the ballooning space. Here, “local” means the ITG eigenmode equation is solved along the magnetic field lines, while physics associated with radial envelope modulation are neglected systematically.

The rest of the paper is organized as follows. In section II, the theoretical model and governing equations are presented. In section III, we analyzed the nonlinear generation of ZS in detail. In section IV, we incorporated the description of beat-driven ZS into the existing linear dispersion relation to investigate the “nonlinear” effects on ITG linear stability. In section V, analytical and numerical results are discussed in both the short- and long-wavelength limits. Finally, a brief summary and discussions are given in section VI.

II. THEORETICAL MODEL

For simplicity and clarity of discussion, we consider a low- β tokamak with large aspect ratio and concentric circular magnetic surfaces, in which the equilibrium magnetic field is given by $\mathbf{B} = B_0 [\mathbf{e}_\zeta / (1 + \varepsilon \cos \theta) + \varepsilon \mathbf{e}_\theta / q]$. Here, $\varepsilon \equiv r/R < 1$ is the inverse aspect ratio, r and R are, respectively, the minor and major radii of the torus, $\beta \equiv 8\pi P/B_0^2 \sim \mathcal{O}(\varepsilon^2) \ll 1$ is the ratio between plasma and magnetic pressure, ζ and θ are the toroidal and poloidal angles, respectively, and $q \equiv rB_\zeta / (RB_\theta)$ is the safety factor. To simplify the analysis while focusing on main physics, the equilibrium distribution functions of thermal plasmas are taken as local Maxwellian, while trapped particle effects are systematically neglected. We take $\delta\phi$ and δA_\parallel as the field variables in the low- β limit, where $\delta\phi$ is the scalar potential and δA_\parallel is the parallel component of vector potential, i.e., $\delta \mathbf{A} \simeq \delta A_\parallel \mathbf{b}$ and $\mathbf{b} \equiv \mathbf{B}/B$ is the unit vector along equilibrium magnetic field. An alternative field variable $\delta\psi \equiv \omega \delta A_\parallel / (ck_\parallel)$ is also adopted for $n \neq 0$ TAEs, and one has $\delta\psi = \delta\phi$ in the ideal MHD limit.

In gyrokinetic theory, the perturbed distribution function, δf_s , with the subscript s representing the particle species $s =$

e, i , can be denoted as

$$\delta f_s = - \left(\frac{e}{T} \right)_s \delta\phi F_{Ms} + \exp(-\rho_s \cdot \nabla) \delta H_s, \quad (1)$$

and its non-adiabatic component δH_s obeys the nonlinear gyrokinetic equation⁴⁰

$$\begin{aligned} (\partial_t + v_\parallel \partial_l + i\omega_{Ds}) \delta H_s = & -i \left(\frac{e}{T} \right)_s (\omega - \omega_*^l) F_{Ms} J_k \delta L_k \\ & - \sum_{\mathbf{k}=\mathbf{k}'+\mathbf{k}''} \Lambda_{k''}^{k'} J_{k'} \delta L_{k'} \delta H_{k''}. \end{aligned} \quad (2)$$

Here, F_{Ms} is the Maxwellian distribution representing equilibrium thermal particle distribution, $\rho_s = \mathbf{b} \times \mathbf{v} / \omega_{cs}$ is the Larmor radius with $\omega_{cs} \equiv eB_0 / (m_s c)$ being the cyclotron frequency, l is the arc length along the equilibrium magnetic field line, $\omega_{Ds} = 2\hat{\omega}_{ds} C$ represents the magnetic drift frequency, with $\hat{\omega}_{ds} \equiv \omega_{ds} (x_\perp^2 / 2 + x_\parallel^2)$, $\omega_{ds} \equiv k_\theta c T_s / (e_s B_0 R)$, $x_\perp = v_\perp / v_{ts}$ and $x_\parallel = v_\parallel / v_{ts}$ being the particle perpendicular/parallel velocities normalized by thermal velocity $v_{ts} \equiv \sqrt{2T_s / m_s}$, respectively, and $C \equiv \cos \theta - \sin \theta k_r / k_\theta$ is related to the magnetic curvature, with k_r and $k_\theta = -m_0 / r_0$ being the radial/poloidal wavenumbers. Furthermore, $\omega_*^l \equiv \omega_{*s} (1 + \eta_s (v^2 / v_{ts}^2 - 3/2))$ is the diamagnetic drift frequency associated with plasma nonuniformity, with $\omega_{*s} = k_\theta c T_s / (e_s B_0 L_n)$, $\eta_s = L_{ns} / L_{Ts}$, where $L_n \equiv -N / (\partial N / \partial r)$, $L_T \equiv -T / (\partial T / \partial r)$ are the characteristic lengths of density and temperature nonuniformities, respectively, $J_k = J_0(k_\perp \rho_s)$ is the Bessel function of zero index accounting for finite Larmor radius (FLR) effects and $k_\perp = \sqrt{k_r^2 + k_\theta^2}$ is perpendicular wavenumber. Furthermore, $\Lambda_{k''}^{k'} \equiv (c/B_0) \mathbf{b} \cdot (\mathbf{k}'' \times \mathbf{k}')$, with $\sum_{\mathbf{k}=\mathbf{k}'+\mathbf{k}''} \Lambda_{k''}^{k'}$ representing the selection rule of frequency and wavenumber matching conditions for nonlinear mode coupling, $\delta L_k \equiv \delta\phi_k - k_\parallel v_\parallel \delta\psi_k / \omega_k$ is the scalar potential in guiding-center moving frame, and other notations are standard. In the following analysis, the non-adiabatic particle response δH_s can be separated into linear and nonlinear components, i.e., $\delta H \equiv \delta H^L + \delta H^{NL}$, with the superscripts “L” and “NL” denoting the linear and nonlinear components, respectively, and can be derived perturbatively assuming $\delta H^{NL} \ll \delta H^L$.

In the $\beta \ll 1$ limit with negligible magnetic compression, the nonlinear gyrokinetic equation can be closed by charge quasi-neutrality

$$\frac{Ne^2}{T_i} \left(1 + \frac{1}{\tau} \right) \delta\phi_k = \sum_s \langle e_s J_k \delta H_k \rangle, \quad (3)$$

and parallel Ampere’s law

$$-\frac{c}{4\pi} \nabla_\perp^2 \delta A_\parallel = \delta J_\parallel = \langle -ev_\parallel \delta f_e \rangle. \quad (4)$$

Here, terms on the left hand side of equation (3) are contributions from adiabatic responses of ion and electron, respectively, $\tau \equiv T_e / T_i$ is the electron to ion temperature ratio, and $\langle \dots \rangle$ represents velocity space integration.

We now consider the effects of indirect modulation of ITG stability by finite amplitude TAE, mediated by beat-driven ZS. More specifically, this is a two-step process, with the first process being finite amplitude TAE $\Omega_0(\omega_0, k_{\theta 0})$ couples with its complex conjugate $\Omega_0^*(-\omega_0, -k_{\theta 0})$ to generate ZS $\Omega_Z(\omega_Z, k_{rZ})$ with $\omega_Z \approx 0$, $k_{\parallel Z} = 0$, $k_{\theta Z} = 0$, and finite k_{rZ} , which is analysed in section III. In the second process, the beat-driven ZS affects the linear stability of ITG $\Omega_I(\omega_I, k_{\theta I})$, and is analyzed in section IV. Here, the subscripts 0, Z and I denote quantities associated with the TAE, ZS and ITG, respectively. For DWs, especially ITG, with most unstable modes characterized with high mode numbers, and the characteristic scale of equilibrium profile variation generally much larger than the distance between neighbouring mode rational surfaces, the well-known ballooning-mode decomposition⁴¹ can be adopted to decompose the two-dimensional eigenvalue problem into two coupled one-dimensional eigenvalue problems, i.e.,

$$\delta\phi_I = A_I e^{-in\zeta - i\omega t} \sum_j \Phi_I(x-j) e^{i(m_0+j)\theta} + c.c. \quad (5)$$

Here, A_I is the radial envelope of ITG, n is the toroidal mode number, $(m = m_0 + j)$ is the poloidal mode number with m_0 being its reference value satisfying $nq(r_0) = m_0$, and r_0 denotes the plasma radial position about which the ITG is assumed to be localized. Furthermore, $x = nq - m_0 \simeq nq'(r - r_0)$, $|j| \ll m_0$ is an integer, and $\Phi_I(x-j)$ is the fine radial structure due to finite k_{\parallel} , with $\int |\Phi_I|^2 dx = 1$ being normalization condition. In the present analysis, we however, will focus on the local stability of ITG, as the ZS driven by TAE are expected to have a larger radial scale than ITG¹¹. The global problem with the radial envelope modulation will be analyzed in a future publication.

III. NONLINEAR ZS GENERATION

In this section, based on the gyrokinetic theoretic framework, i.e., equations (2)-(4), the nonlinear generation of ZS by TAEs self-beating is investigated. Briefly speaking, the particle responses to ZS due to TAE self-coupling (i.e., PSZS) are derived from the nonlinear gyrokinetic equation, which are then substituted into the quasi-neutrality condition and parallel Ampere's law to derive the zonal scalar and vector potential response, which then will be used to study the TAE effects on ITG via ZS mediation in section IV.

We start from the linear particle response to the finite amplitude TAE $\Omega_0(\omega_0, k_{\theta 0})$, which will be used in the nonlinear term of the gyrokinetic equation later. For massless-electron with $|k_{\parallel} v_{te}/\omega_0| \gg 1$, $|k_{\perp} \rho_e| \ll 1$ and $J_0(k_{\perp} \rho_e) \sim 1$ satisfied, the linear electron response to Ω_0 can be straightforwardly derived as

$$\delta H_{0,e}^L \simeq -\frac{e}{T_e} \left(1 - \frac{\omega_{*e,0}^t}{\omega_0} \right) F_{Me} \delta\psi_0. \quad (6)$$

Meanwhile, for ions with $|k_{\parallel} v_{ti}/\omega_0| \ll 1$, we have

$$\delta H_{0,i}^L \simeq \frac{e}{T_i} \left(1 - \frac{\omega_{*i,0}^t}{\omega_0} \right) F_{Mi} J_0 \delta\phi_0. \quad (7)$$

Substituting above expressions into the quasi-neutrality condition and vorticity equation⁷, the dispersion relation of TAE can be obtained. In our analysis focusing on TAE effects on ITG stability, we however, do not need the detailed expression of TAE dispersion relation.

The linear and nonlinear particle responses to ZS can be derived by transforming equation (2) into drift orbit center coordinate, i.e., taking $\delta H_{Z,s} \equiv \delta H_{dZ,s} \exp(i\lambda_Z)$, with $\lambda_Z \equiv \hat{\lambda}_{dZ} \cos \theta$ satisfying $\omega_{tr} \partial_{\theta} \lambda_Z + \omega_{Drs} = 0$, and $\hat{\lambda}_{dZ} \equiv -2\hat{\omega}_{dr}/\omega_{tr}$ being the normalized drift orbit width. Here, $\omega_{tr} \equiv v_{\parallel}/qR$ is the transit frequency, $\omega_{Drs} \equiv -2\hat{\omega}_{drs} \sin \theta$, and $\hat{\omega}_{drs} \equiv k_r c T_s (x_{\perp}^2/2 + x_{\parallel}^2)/(e_s B_0 R)$. Substituting $\delta H_{Z,s}$ into equation (2), we have

$$\begin{aligned} (\partial_t + \omega_{tr} \partial_{\theta}) \delta H_{dZ} &= -i \left(\frac{e}{T} \right)_s e^{-i\lambda_Z} \omega_Z F_{Ms} J_Z \left(\delta\phi - \frac{v_{\parallel}}{c} \delta A \right)_Z \\ &\quad - \sum_{\mathbf{k}=\mathbf{k}'+\mathbf{k}''} e^{-i\lambda_Z} \Lambda_{\mathbf{k}''}^k J_{\mathbf{k}'} \delta L_{\mathbf{k}'} \delta H_{\mathbf{k}''}. \end{aligned} \quad (8)$$

Noting the $v_{ts}/(qR) \gg \omega_Z$ ordering for both electrons and ions, and taking the dominant flux surface averaged quantities $\overline{(\dots)} \equiv \int_0^{2\pi} (\dots) d\theta / (2\pi)$, the linear particle response to Ω_Z can be straightforwardly derived from the linear term of equation (8) as

$$\overline{\delta H_{Z,e}^L} \simeq -\frac{e}{T_e} F_{Me} \left(\delta\phi - \frac{v_{\parallel}}{c} \delta A \right)_Z, \quad (9)$$

$$\overline{\delta H_{Z,i}^L} = \frac{e}{T_i} F_{Mi} J_Z |\theta_Z|^2 \left(\delta\phi - \frac{v_{\parallel}}{c} \delta A \right)_Z, \quad (10)$$

where $\theta_Z \equiv e^{-i\lambda_Z}$. Meanwhile, noting the linear particle responses to TAE given in equations (6) and (7), the nonlinear particle response to Ω_Z can be derived as

$$\overline{\delta H_{Z,e}^{NL}} = -\frac{c}{B_0} k_{\theta 0} \frac{e}{T_e} F_{Me} \left(\frac{\omega_{*e,0}^t}{\omega_0^2} - \frac{k_{\parallel 0} v_{\parallel}}{\omega_0^2} \right) \partial_r |\delta\phi_0|^2, \quad (11)$$

$$\overline{\delta H_{Z,i}^{NL}} = \frac{c}{B_0} |\theta_Z|^2 k_{\theta 0} \frac{e}{T_i} J_0^2 F_{Mi} \frac{\omega_{*i,0}^t}{\omega_0^2} \partial_r |\delta\phi_0|^2, \quad (12)$$

where $\partial_r = ik_{rZ}$ is the operator for radial derivative. It is reasonable to conclude from equations (11) and (12) that, $\partial_r |\delta\phi_0|^2 \sim ik_{rZ} |\delta\phi_0|^2$, corresponding to the fine scale ZS generation by weakly/moderately ballooning TAE¹¹. Substituting the particle responses to Ω_Z into the quasi-neutrality condition, nonlinear equation of zonal scalar potential generation by TAE in nonuniform plasmas can be derived as

$$\begin{aligned} \delta\phi_Z &= \frac{c}{B_0} k_{\theta 0} \frac{\omega_{*i,0}^t}{\omega_0^2} \left[\frac{\eta_i}{\chi_{iZ}} \left\langle \frac{F_{Mi}}{n_0} J_Z |\theta_Z|^2 J_0^2 \right. \right. \\ &\quad \left. \left. \times \left(\frac{v^2}{v_{ti}^2} - \frac{3}{2} \right) \right\rangle - 1 \right] \partial_r |\delta\phi_0|^2. \end{aligned} \quad (13)$$

Here, $\chi_{iZ} \equiv 1 - \langle F_{Mi}/n_0 J_Z^2 |\theta_Z|^2 \rangle \approx 1.6 k_{rZ}^2 \rho_{Ti}^2 q^2 / (2\sqrt{\epsilon})$ is the well known neoclassical inertia enhancement dominated by trapped particle contribution²⁷, and $\rho_{Ti} \equiv v_{Ti}/\omega_{ci}$ is the ion Larmor radius defined by ion thermal velocity. If we neglect the FLR effects by taking $J_Z(k_{rZ}\rho_i) \simeq 1$, noting that, $\langle F_{Mi}/n_0 |\theta_Z|^2 (v^2/v_{Ti}^2 - 3/2) \rangle = -\chi_{iZ}$, equation (13) can be explicitly written as

$$\delta\phi_Z = -\frac{c}{B_0} k_{\theta 0} \frac{\omega_{*pi,0}}{\omega_0^2} \partial_r |\delta\phi_0|^2. \quad (14)$$

Here, $\omega_{*pi} \equiv \omega_{*i} + \omega_{*Ti}$ with $\omega_{*Ti} = \eta_i \omega_{*i}$. Equation (14) describes ZF beat-driven by TAE, different from the spontaneous excitation process described in Ref. 31. It is noteworthy that, equation (14) illustrates that the growth rate of the beat-driven zonal scalar potential is twice that of the TAE instantaneous growth rate, and its magnitude being proportional to the intensity of the TAE. This is a typical feature of the beat-driven process^{35,37,42}, with the crucial role played by the nonlinear ion response to ZF due to thermal ion nonuniformity. The beat-driven process is thresholdless, significantly different from the spontaneous excitation process via modulational instability of TAE, which requires a sufficiently large TAE amplitude to overcome the threshold due to frequency mismatch¹¹. This is the reason why the beat-driven process is universally observed in simulations^{35,36,42,43}.

Meanwhile, the equation for zonal current generation can be derived from the parallel component of Ampere's law³¹. One obtains from the zonal component of equation (4),

$$\delta A_{\parallel Z} \simeq -\frac{c^2}{B_0} k_{\theta 0} \frac{k_{\parallel 0}}{\omega_0^2} \partial_r |\delta\phi_0|^2, \quad (15)$$

with the assumption of $k_{\perp}^2 c^2 / \omega_{pe}^2 \ll 1$, and $\omega_{pe}^2 = 4\pi n_0 e^2 / m_e$ being the electron plasma frequency. Equations (14)-(15), together with nonlinear particle response to ZS given by equations (11)-(12) (i.e., PSZS), will be used to study TAE effects on ITG via ZS mediation in section IV.

IV. EFFECTS OF BEAT-DRIVEN ZS ON DW LINEAR STABILITY

Next, we consider the effects of beat-driven ZS on ITG linear stability. For simplicity, we consider the ITG to be electrostatic, and the analysis follows closely that of Ref. 39. The ITG equation is derived from quasi-neutrality condition, i.e., equation (3), with the particle responses derived from nonlinear gyrokinetic equation.

For ITG with $k_{\parallel} v_{Te} \gg \omega \sim \omega_{*i} \gg \omega_{Ds}$, the linear electron response to ITG is adiabatic, i.e.,

$$\delta H_{I,e}^L \approx 0;$$

and for ion with $\omega \gg k_{\parallel} v_{Ti}$, the linear ion responses to ITG can be derived as

$$\delta H_{I,i}^L \simeq \frac{e}{T_i} \left(1 - \frac{\omega_{*i}}{\omega}\right) \left(1 + \frac{v_{\parallel} k_{\parallel}}{\omega} + \frac{v_{\parallel}^2 k_{\parallel}^2}{\omega^2} + \frac{\omega_{Di}}{\omega}\right) F_{Mi} J_0 \delta\phi_I.$$

Here, we have adopted the fluid-ion approximation in order to simplify the analysis and, thereby, illustrate more clearly the effects of ZS on ITG stabilizing. Substituting the linear particle responses to ITG into quasi-neutrality condition, the linear ITG equation can be derived as

$$\epsilon_I \delta\phi_I = 0, \quad (16)$$

with

$$\epsilon_I = 1 - \frac{\omega_{*e}}{\omega} + \tau \left(1 - \frac{\omega_{*pi}}{\omega}\right) \left(b_{\perp} - \frac{k_{\parallel}^2 v_{Ti}^2}{2\tau\omega^2} - \frac{2\omega_{di}C}{\omega}\right) \quad (17)$$

being the linear ITG dielectric operator, and $b_{\perp} = k_{\perp}^2 \rho_i^2 / 2$. The contributions of beat-driven ZS, enter through the formally "nonlinear" terms, including scattering by zonal field structure (i.e., $\delta\phi_Z$ and $\delta A_{\parallel Z}$) via $J_Z \delta L_Z \delta H_I$ and nonlinear modification of equilibrium by PSZS via $J_I \delta\phi_I \delta H_Z^{NL}$ in the nonlinear gyrokinetic equation

$$(\partial_t + v_{\parallel} \partial_I + i\omega_D) \delta H_I^{NL} = \Lambda [J_I \delta\phi_I (\delta H_Z^L + \delta H_Z^{NL}) - J_Z \delta L_Z \delta H_I^L], \quad (18)$$

with $\Lambda = -ck_{rZ}k_{\theta I}/B_0$. Noting the $k_{\parallel} v_{Te} \gg \omega \gg k_{\parallel} v_{Ti}$ ordering again, we have

$$\delta H_{I,e}^{NL} \simeq 0, \quad (19)$$

and

$$\delta H_{I,i}^{NL} = \frac{e}{T_i} F_{Mi} \left[\left(|\theta_Z|^2 - 1 + \frac{\omega_{*i}}{\omega} \right) \frac{\omega_{*pi}}{\omega} - \frac{\omega_{*i}}{\omega} |\theta_Z|^2 \right] \delta \hat{\phi}_0^2 \delta\phi_I. \quad (20)$$

Here, $\delta \hat{\phi}_0^2 = |ck_{\theta 0}/(B_0 \omega_0)|^2 \partial_r^2 |\delta\phi_0|^2$. Note that $\delta \hat{\phi}_0$ is related to the normalized Doppler shift induced by radial electric field of TAE, and is also related to the beat-driven ZF induced shearing rate. In deriving equations (19) and (20), we neglected the FLR effects by taking $J_Z(k_{rZ}\rho_i) \simeq 1$, and the expressions of the beat-driven ZS given by equations (11), (12), (14) and (15) are used. Substituting equations (19) and (20) into the quasi-neutrality condition, the equation describing nonlinear modulation of ITG by the beat-driven ZS can be written as

$$\frac{n_0 e^2}{T_e} \left[\epsilon_I + \tau \frac{\omega_{*i}}{\omega} \left(1 - \frac{\omega_{*pi}}{\omega}\right) \delta \hat{\phi}_0^2 \right] \delta\phi_I = 0. \quad (21)$$

Combining equations (17) and (21), one then has the ITG dispersion relation in the WKB limit

$$\left[\frac{\omega}{\tau(\omega - \omega_{*pi})} + \frac{\omega_{*i}}{\omega - \omega_{*pi}} + b_{\perp} - \frac{k_{\parallel}^2 v_{Ti}^2}{2\omega^2} - \frac{2\omega_{di}C}{\omega} + \frac{\omega_{*i}}{\omega} \delta \hat{\phi}_0^2 \right] \delta\phi_I = 0. \quad (22)$$

Here, operators ω , b_{\perp} and k_{\parallel} without subscripts $k=0, Z$ represent ITG. The first five terms of equation (22) constitute the

linear ITG dispersion relation, which deviates slightly from that in Ref. 39, primarily due to the inclusion of both density and temperature nonuniformities in the present analysis, while Ref. 39 took the flat density gradient limit to focus on the effects of ion temperature gradient, following the early analysis of Ref. 44. Moreover, the first four terms correspond to the adiabatic electron response, ion $\mathbf{E} \times \mathbf{B}$ drift, the FLR effect (polarization), and the parallel compressibility, respectively. The fifth term accounts for the magnetic drift, which is unique to toroidal configurations and leads to the coupling of adjacent poloidal harmonics. The last term introduces a nonlinear modification attributed to the beat-driven ZS, and is the main novel contribution of the present work. Additionally, in this context, the final term represents a nonlinear correction that takes into account the combined contributions of ZF, ZC, and PSZS. The contribution of each of the three components to the nonlinear ITG dispersion relation will be presented in the Appendix A.

Noting $k_{\perp}^2 = k_{\theta}^2 - \partial^2/\partial r^2$, and introducing the Fourier transform $\Phi(\eta) = \int \Phi(nq - m) \exp(-i\eta(nq - m)) d(nq - m)$ with $nq - m$ being the normalized distance to the mode rational surface and $\Phi(nq - m)$ being the poloidal harmonic of ITG, the ITG eigenmode equation in ballooning space can be derived as

$$\begin{aligned} & \frac{d^2\Phi(\eta)}{d\eta^2} + q^2\Omega^2b \left[-\frac{\tau}{(1 + \tau\Omega\varepsilon_{pi}^{1/2})(1 + \eta_i)\varepsilon_{pi}^{1/2}} \right. \\ & + \frac{\tau\Omega}{1 + \tau\Omega\varepsilon_{pi}^{1/2}} + b(1 + \hat{s}^2\eta^2) + \frac{2}{\Omega}(\cos\eta + \hat{s}\eta\sin\eta) \\ & \left. - \frac{1}{\Omega\varepsilon_{pi}(1 + \eta_i)}\delta\hat{\phi}_0^2 \right] \Phi(\eta) = 0, \end{aligned} \quad (23)$$

where $\hat{s} \equiv r(\partial q/\partial r)/q$ denotes the magnetic shear, $\Omega \equiv \omega/(\tau\sqrt{\omega_{*pi}\omega_{di}})$, $b \equiv \tau b_{\theta}/\sqrt{\varepsilon_{pi}}$, and $\varepsilon_{pi} \equiv L_{pi}/R$. Equation (23) is the paradigmatic one-dimensional eigenvalue equation with the potential well contributed by two components: a slowly varying parabolic well stemming from the FLR effect $(1 + \hat{s}^2\eta^2)$, and a rapidly oscillating periodic well due to magnetic curvature $(\cos\eta + \hat{s}\eta\sin\eta)$, while the beat-driven ZS by TAE enter the ITG eigenmode equation by modifying the potential well depth while not affecting the parity or periodicity. These distinct potential wells result in two principal ITG eigenmode branches: the slab branch sensitive to the slow parabolic variation $(1 + \hat{s}^2\eta^2)$, and the toroidal branch due to the rapid periodic fluctuations $(\cos\eta + \hat{s}\eta\sin\eta)$. In section V, following the analysis of Refs. 45 and 46, we assess the impact of ZS on ITG characteristics, including frequency, growth rate, and mode structure, in the short- and long-wavelength regimes, respectively. The analytical results are then compared with numerical solution of equation (23) using the eigenmatrix method. In equation (23), we also note that $\delta\hat{\phi}_0^2 = |ck_{\theta 0}/(B_0\omega_0)|^2 \partial_r^2 |\delta\phi_0|^2 \sim -|k_{rZ}/k_{||0}|^2 |\delta B_r/B_0|^2$, assuming the TAE is close to ideal MHD condition. Taking typical tokamak parameters, i.e., $k_{rZ} \sim 1/\rho_E$, $k_{||0} \sim 1/(2qR)$, and $|\delta B_r/B_0|^2 \leq 2.5 \times 10^{-7}$ for TAE fluctuations level expected in reactors⁴⁷, we then find

$$\delta\hat{\phi}_0^2 \sim \mathcal{O}(10^{-1}), \text{ and } e\delta\phi_Z/T_i \leq 5 \times 10^{-4}.$$

V. ANALYTICAL AND NUMERICAL RESULTS

In this section, we follow the theoretical approach of Refs. 45 and 46, and investigate the impact of TAE-driven-ZS on ITG linear stability in both short- and long-wavelength limits, corresponding to strong and moderate ballooning cases, respectively. The two limiting parameter regimes, can be studied by taking $b \sim \mathcal{O}(1)$ and $b \ll 1$, respectively, which is given *a priori*, and will be shown below.

A. Short-wavelength limit

In the short-wavelength limit, i.e., $b \sim \mathcal{O}(1)$, the parallel mode structure of ITG is strongly localized in ballooning space⁴⁵. Assuming that the ITG eigenmode is localized around $\eta = 0$ in the ballooning space, in which strong coupling approximation can be adopted by taking $\cos\eta \approx 1 - \eta^2/2$ and $\sin\eta \approx \eta$, and the ITG eigenmode equation becomes

$$\begin{aligned} & \frac{d^2\Phi(\eta)}{d\eta^2} + q^2\Omega^2b \left[-\frac{\tau}{(1 + \tau\Omega\varepsilon_{pi}^{1/2})(1 + \eta_i)\varepsilon_{pi}^{1/2}} \right. \\ & + \frac{\tau\Omega}{1 + \tau\Omega\varepsilon_{pi}^{1/2}} + b + \frac{2}{\Omega} - \frac{1}{\Omega\varepsilon_{pi}(1 + \eta_i)}\delta\hat{\phi}_0^2 \\ & \left. + \left(b\hat{s}^2 + \frac{2\hat{s}-1}{\Omega} \right) \eta^2 \right] \Phi(\eta) = 0, \end{aligned} \quad (24)$$

which can be rewritten as a standard Weber equation with the most unstable ground eigenmode given by $\delta\phi = \exp(-\sigma\eta^2)$, with

$$\begin{aligned} \sigma = & \frac{q^2\Omega^2b}{2} \left[-\frac{\tau}{(1 + \tau\Omega\varepsilon_{pi}^{1/2})(1 + \eta_i)\varepsilon_{pi}^{1/2}} \right. \\ & \left. + \frac{\tau\Omega}{1 + \tau\Omega\varepsilon_{pi}^{1/2}} + b + \frac{2}{\Omega} - \frac{1}{\Omega\varepsilon_{pi}(1 + \eta_i)}\delta\hat{\phi}_0^2 \right]. \end{aligned} \quad (25)$$

The half width of the ground-state eigenmode in ballooning space is proportional to $1/\sqrt{b}$, and consequently, it is proportional to \sqrt{b} in real space, consistent with the strong coupling approximation. The corresponding dispersion relation is

$$\begin{aligned} & q^2\Omega^2b \left[-\frac{\tau}{(1 + \tau\Omega\varepsilon_{pi}^{1/2})(1 + \eta_i)\varepsilon_{pi}^{1/2}} \right. \\ & + \frac{\tau\Omega}{1 + \tau\Omega\varepsilon_{pi}^{1/2}} + b + \frac{2}{\Omega} - \frac{1}{\Omega\varepsilon_{pi}(1 + \eta_i)}\delta\hat{\phi}_0^2 \left. \right]^2 \\ & + \left(b\hat{s}^2 + \frac{2\hat{s}-1}{\Omega} \right) = 0. \end{aligned} \quad (26)$$

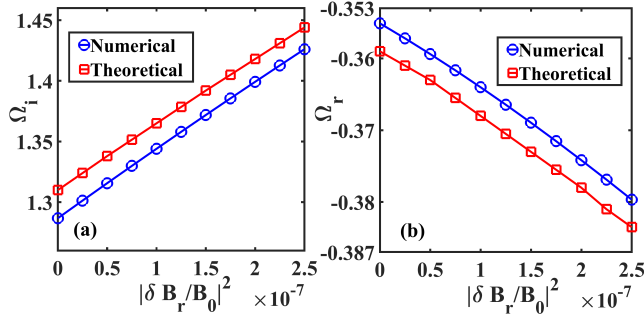


FIG. 1. The dependence of normalized ITG growth rate (a) and real frequency (b) vs TAE amplitude in short-wavelength limit. The squares represent the theoretical result given by equation (26) while circles are numerical results of equation (23). Here, $\eta_i = 2$, $\varepsilon_{pi} = 0.06$, $q = 1$ and $b = 1$.

The dependence of ITG growth rate and real frequency on the amplitude of ZS is solved from the theoretical dispersion relation equation (26), which are then compared with the numerical solution of equation (23), as shown in FIG. 1.

Good agreement between analytical and numerical results are obtained. It is found that, the ITG real frequency as well as growth rate change only slightly with TAE amplitude with the typical tokamak parameters regime, i.e., $|\delta B_r/B_0|^2 \leq 2.5 \times 10^{-7}$. More importantly, the ITG growth rate increases with TAE amplitude, suggesting the ZS beat driven by TAE, has only weakly destabilizing effect on ITG stability, contrary to the general speculation. In particular, the influence of ZS on the ITG in our work is significantly less pronounced than the results reported in Ref. 39, where effects of radial electric field from electro-static ZFZF on ITG stability are investigated. This discrepancy primarily stems from the coefficient of the nonlinear term in our equation (23) being substantially smaller than the corresponding coefficient in equation (7) of Ref. 39. In fact, even at the maximum TAE amplitude adopted, the amplitude of the ZS beat-driven by TAE is also quite small, i.e., $e\delta\phi_z/T_i \leq 5 \times 10^{-4}$, so it is reasonable that the impact of the TAE beat-driven ZS on the ITG linear stability is correspondingly weak. If the coefficient of the nonlinear term is artificially enlarged by a factor of five, as depicted by the magenta dotted line in FIG. 2, the destabilizing effect of TAE beat-driven ZS on ITG becomes markedly evident. Besides, in present work, linear growth rate of ITG increase with TAE amplitude, which is in contrast to the numerical results in Ref. 39. The primary reason is attributed to the difference in the sign of the nonlinear terms, which is opposite to that in Ref. 39. As the sign of the nonlinear term in Equation (23) is artificially reversed, as illustrated by the red long dashed line in FIG. 2, the ITG growth rate decreases with TAE amplitude, similar to the results of Ref. 39. However, the underlying physical mechanisms remain elusive and is worthy of further investigation.

The corresponding mode structures of the most unstable mode are shown in FIG. 3, where the blue dotdash curve represents the case with $|\delta B_r/B_0|^2 = 2.5 \times 10^{-7}$, red-dashed and magenta dotted curves represent the cases with the nonlin-

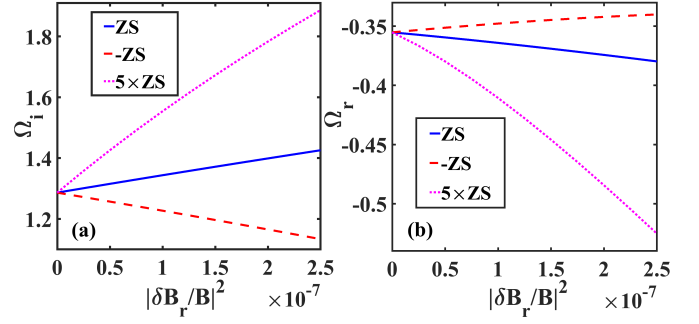


FIG. 2. The dependence of normalized ITG growth rate (a) and real frequency (b) vs TAE amplitude in short-wavelength limit. Here, $\eta_i = 2$, $\varepsilon_{pi} = 0.06$, $q = 1$ and $b = 1$.

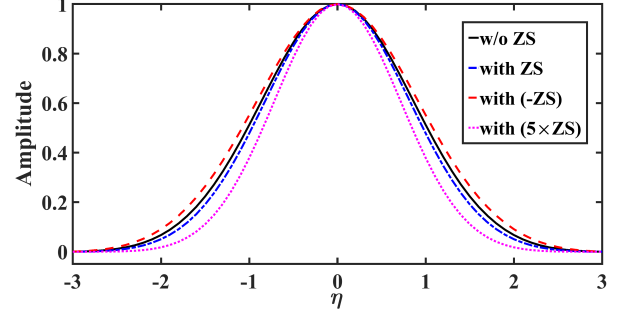


FIG. 3. The mode structures of the most unstable mode with different ZS values. Here, $\varepsilon_{pi} = 0.06$, $q = 1$ and $b = 1$.

ear term artificially changed sign and increased by 5 times, respectively; and the black curve represents the linear mode structure. Clearly, the TAE beat-driven ZS reduces the half-width of the most unstable ITG mode structure. However, even at the maximum amplitude of TAE, the impact of the TAE thermally driven ZS on the ITG mode structure remains minimal. The primary reason is that the TAE beat-driven ZS slightly reduces the depth of the potential well, thereby decreasing the distance between the turning points of the potential well and localizing the ITG mode within a narrower range of stronger drive at the bad curvature region, as shown in FIG. 4, and this is confirmed by the magenta dotted curve and red dashed curve, where the nonlinear term is artificially changed sign or enlarged by a factor. Additionally, the mode structure peaks at $\eta = 0$ and the even symmetry remains unbroken, a result of the even-symmetric modulation introduced by the beat-driven ZS.

B. Long-wavelength limit

For typical tokamak plasmas, strong coupling approximation is usually a rough approximation. In more general cases, long wavelength limit with $b \ll 1$ is satisfied⁴⁶. In the long-wavelength limit, there are two branches, i.e., the toroidal branch and the slab branch. We are more concerned about the toroidal branch⁴⁶, which is characterized by fast varia-

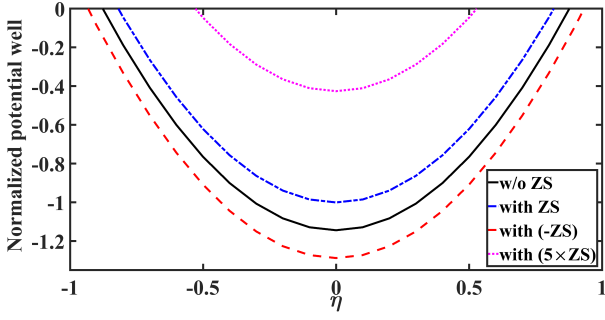


FIG. 4. Potential wells with different values of ZS. Here, $\varepsilon_{pi} = 0.06$, $q = 1$ and $b = 1$.

tion over connection length scale ($\eta \sim \mathcal{O}(1)$) and a superimposed slowly varying envelope over secular scale. Following the analysis of Ref. 46, taking $\Phi(\eta) = C_0(\eta_1) \cos \eta/2 + S_0(\eta_1) \sin \eta/2$ with $\eta_1 \equiv \hat{\varepsilon}\eta$ and $\hat{\varepsilon} = b^{1/3}$ denoting slow variation in η , the eigenmode equations can be derived from vanishing coefficients of the linearly independent bases $\sin \eta/2$ and $\cos \eta/2$,

$$\frac{dS_0}{d\eta_1} + \left[\frac{q^2 b^{2/3} \Omega^3 \tau}{1 + \tau \Omega \varepsilon_{pi}^{1/2}} - \frac{q^2 b^{2/3} \Omega^2 \tau}{(1 + \tau \Omega \varepsilon_{pi}^{1/2})(1 + \eta_i) \varepsilon_{pi}^{1/2}} - \frac{1}{4b^{1/3}} - \frac{q^2 b^{2/3} \Omega}{\varepsilon_{pi}(1 + \eta_i)} \delta \hat{\phi}_0^2 \right] C_0 + q^2 \Omega b^{1/3} \hat{s} \eta_1 S_0 = 0, \quad (27)$$

$$\frac{dC_0}{d\eta_1} - \left[\frac{q^2 b^{2/3} \Omega^3 \tau}{1 + \tau \Omega \varepsilon_{pi}^{1/2}} - \frac{q^2 b^{2/3} \Omega^2 \tau}{(1 + \tau \Omega \varepsilon_{pi}^{1/2})(1 + \eta_i) \varepsilon_{pi}^{1/2}} - \frac{1}{4b^{1/3}} - \frac{q^2 b^{2/3} \Omega}{\varepsilon_{pi}(1 + \eta_i)} \delta \hat{\phi}_0^2 \right] S_0 - q^2 \Omega b^{1/3} \hat{s} \eta_1 C_0 = 0. \quad (28)$$

Equation (27) and (28) can be cast into a Weber equation for C_0 and S_0 , which then yields the dispersion relation for the most unstable ground eigenstate

$$\Omega^3 - \Omega^2 \left[\frac{1}{(1 + \eta_i) \varepsilon_{pi}^{1/2}} - \frac{1}{(1 + \eta_i) \varepsilon_{pi}^{1/2}} \delta \hat{\phi}_0^2 \right] \times \left(1 + \frac{1}{\tau \Omega \varepsilon_{pi}^{1/2}} \right) = \frac{1}{4bq^2 \tau} (1 + \tau \Omega \varepsilon_{pi}^{1/2}). \quad (29)$$

The dispersion relation is similar to corresponding linear result⁴⁶, with the term proportional to $\delta \hat{\phi}_0^2$ originating from the contribution of beat-driven ZS.

Following the same procedures, the dependence of the ITG growth rate and real frequency on beat-driven ZS in the long-wavelength limit is illustrated in FIG. 5. Analytical and numerical results indicate that in the long-wavelength limit, the growth rate as well as real frequency of the toroidal branch vary in a similar manner to the results of the short-wavelength limit. That is, the ITG growth rate slightly increases with TAE amplitude, indicating that ZS beat-driven by TAE has

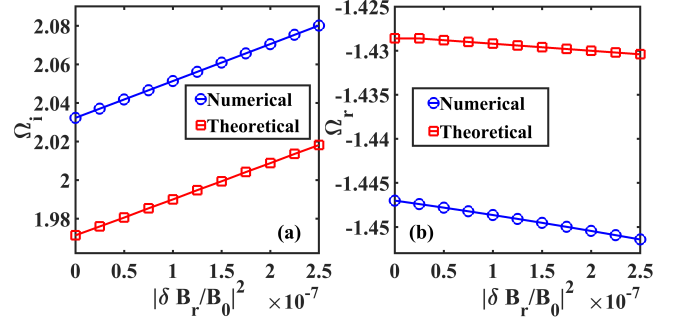


FIG. 5. The dependence of normalized ITG growth rate (a) and real frequency (b) vs the TAE amplitude in long-wavelength limit. The squares represent the theoretical result given by equation (29) while circles are numerical results of equation (23). Here, $\eta_i = 2$, $\varepsilon_{pi} = 0.06$, $q = 1$ and $b = 0.01$.

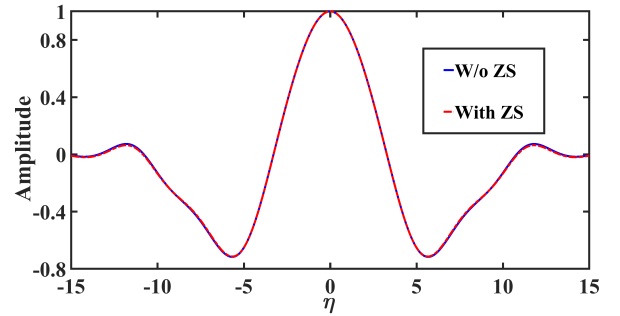


FIG. 6. The mode structure of the most unstable mode. Here, $\varepsilon_{pi} = 0.06$, $q = 1$ and $b = 0.01$.

only a weakly destabilizing effect on ITG stability due to the relatively small amplitude of the ZS, as well as its phase. The analysis methods are similar to those used in the short-wavelength limit, and thus, will not be repeated here. It is noteworthy that, an artificially small $b = 0.01$ is adopted here to separate different scales for analytical progress, due to the weak dependence of $\hat{\varepsilon} \propto b^{1/3}$, although this is not the most relevant parameter regime for ITG stability. The mode structure in the long-wavelength limit is presented in FIG. 6, which indicates clearly that the impact of the TAE beat-driven ZS on the most unstable mode is negligible.

VI. SUMMARY AND DISCUSSION

In this work, the indirect nonlinear interaction between toroidal Alfvén eigenmode (TAE) and ion temperature gradient mode (ITG) is investigated using nonlinear gyrokinetic theory and ballooning formalism, to understand the thermal plasma confinement in the presence of energetic particles (EPs) and the associated electromagnetic oscillations. More specifically, the local stability of ITG in the presence of zonal structures (ZS) beat-driven by finite amplitude TAE is analyzed. The governing ITG eigenmode equation in the ballooning space is derived and solved both analytically and numerically, and it is found that, for typical reactor parameters

and TAE fluctuation level, the ZS beat-driven by TAE has only weakly destabilizing effects on ITG stability in both short- and long-wavelength limits, contrary to the previous speculations. This is due to the relatively weak ZS generation in the parameter region, i.e., $|e\delta\phi_Z/T_i| \sim O(10^{-4})$, partly due to the scale separation between TAE and ITG.

In the present analysis, the contributions of zonal field structure, including zonal flow (ZF), zonal current (ZC), and phase space zonal structure (PSZS) are accounted for on the same footing, and only the overall results are analysed. The respective contributions of zonal field structure and PSZS to the ITG dispersion relation in the WKB limit are provided in the Appendix. However, their respective contribution to the ITG stability are not analysed, as the structure of the corresponding eigenmode equation in the ballooning space is significantly modified, due to the non-vanishing nonlinear electron response to ITG, which makes the comparison to the present results not relevant.

The major assumptions made in the present analysis, include 1. the ZS are beat-driven by TAE, and 2. only the local stability of ITG is investigated. It is noteworthy that, in a previous study, it is found that, the direct scattering of electron drift wave (eDW) by finite amplitude ambient TAE has negligible effects on eDW stability³⁰. The present work, together with Ref. 30, thus, ruled out most channels for the regulation of ITG by ambient electromagnetic oscillations driven by EPs, such as TAE. The potentially effective channels to stabilize DW turbulence, including the spontaneously excited ZS by TAE via modulational instability, as well as DW radial envelope modulation by ZS, are ongoing work of the team, and will be reported in future publications.

ACKNOWLEDGEMENT

This work was supported by the Strategic Priority Research Program of Chinese Academy of Sciences under Grant No. XDB0790000, the National Science Foundation of China under Grant Nos. 12275236 and 12261131622, and Italian Ministry for Foreign Affairs and International Cooperation Project under Grant No. CN23GR02. This work was also supported by the EUROfusion Consortium, funded by the European Union via the Euratom Research and Training Programme (Grant Agreement No. 101052200 EUROfusion). The views and opinions expressed are, however, those of the author(s) only and do not necessarily reflect those of the European Union or the European Commission. Neither the European Union nor the European Commission can be held responsible for them.

Appendix A: Nonlinear contributions of ZFS and PSZS to ITG

Here, we will give the respective contributions of zonal field structure (ZFS, i.e., $\delta\phi_Z$ and $\delta A_{\parallel Z}$) and PSZS (i.e., δH_Z^{NL}) on the ITG linear stability. In the nonlinear gyrokinetic equation

for nonlinear particle response to ITG

$$\begin{aligned} (\partial_t + v_{\parallel} \partial_l + i\omega_D) \delta H_i^{NL} = & \Lambda [J_l \delta \phi_l (\delta H_Z^L + \delta H_Z^{NL}) \\ & - J_Z \left(\delta \phi_Z - \frac{v_{\parallel}}{c} \delta A_{\parallel Z} \right) \delta H_l^L], \end{aligned} \quad (\text{A1})$$

the first and third term in the square bracket on the right hand side are contributions from ZFS (noting that δH_Z^L is related to $\delta\phi_Z$ and $\delta A_{\parallel Z}$), while the second term corresponds to contribution from PSZS.

1. Nonlinear contribution of PSZS to ITG

If only PSZS contribution is kept by taking $\delta\phi_Z = 0$, $\delta A_{\parallel Z} = 0$, it results in $\delta H_Z^L = 0$, the corresponding nonlinear particle response to ITG can be derived as

$$\delta H_{l,e}^{NL} = \frac{e}{T_e} F_{Me} \frac{k_{\theta l}}{k_{\theta 0}} \frac{k_{\parallel 0}}{k_{\parallel l}} \delta \hat{\phi}_0^2 \delta \phi_l, \quad (\text{A2})$$

$$\delta H_{l,i}^{NL} = -\frac{e}{T_i} |\theta_Z|^2 F_{Mi} \frac{\omega_{*i}^l}{\omega} \delta \hat{\phi}_0^2 \delta \phi_l. \quad (\text{A3})$$

Substituting equations (A2) and (A3) into the quasi-neutrality condition, the nonlinear ITG equation in the presence of PSZS beat-driven by TAE can be derived as

$$\begin{aligned} \left[\varepsilon_l - \tau \frac{\omega_{*i}}{\omega} (\chi_{iZ} + \eta_i \chi_{iZ} - 1) \delta \hat{\phi}_0^2 \right. \\ \left. - \frac{k_{\theta l}}{k_{\theta 0}} \frac{k_{\parallel 0}}{k_{\parallel l}} \delta \hat{\phi}_0^2 \right] \delta \phi_l = 0, \end{aligned} \quad (\text{A4})$$

with the term proportional to $\delta \hat{\phi}_0^2$ being the contribution of PSZS beat-driven by TAE.

2. Nonlinear contribution of ZFS to ITG

If we consider only the ZFS contribution by taking $\delta H_Z^{NL} = 0$, one then obtains the nonlinear particle response to ITG as

$$\delta H_{l,e}^{NL} = -\frac{e}{T_e} F_{Me} \frac{k_{\theta l}}{k_{\theta 0}} \frac{k_{\parallel 0}}{k_{\parallel l}} \delta \hat{\phi}_0^2 \delta \phi_l, \quad (\text{A5})$$

$$\delta H_{l,i}^{NL} = \frac{e}{T_i} F_{Mi} \left(|\theta_Z|^2 - 1 + \frac{\omega_{*i}^l}{\omega} \right) \frac{\omega_{*pi}}{\omega} \delta \hat{\phi}_0^2 \delta \phi_l. \quad (\text{A6})$$

Substituting equations (A5) and (A6) into the quasi-neutrality condition, the nonlinear ITG equation can be derived as

$$\begin{aligned} \left[\varepsilon_l - \tau \frac{\omega_{*i}}{\omega} \left(-\chi_{iZ} - \eta_i \chi_{iZ} + \frac{\omega_{*pi}}{\omega} \right) \delta \hat{\phi}_0^2 \right. \\ \left. + \frac{k_{\theta l}}{k_{\theta 0}} \frac{k_{\parallel 0}}{k_{\parallel l}} \delta \hat{\phi}_0^2 \right] \delta \phi_l = 0, \end{aligned} \quad (\text{A7})$$

Equation (22) can be recovered by combining the nonlinear terms of equations (A4) and (A7), i.e., the contributions of PSZS and ZFS. We however, will not compare the results of equations (A4) and (A7) to that of equation (22), as the structures of the equations are very different. More specifically, the

$1/k_{\parallel I}$ terms in equations (A4) and (A7) due to non-vanishing nonlinear electron response to ITG, render the corresponding ITG eigenmode equations into a third order differential equation in ballooning space, whereas equation (22) will yield a second order differential equation in ballooning space, as the terms proportional to $1/k_{\parallel I}$ in equations (A4) and (A7) cancel each other.

REFERENCES

- ¹W. Horton, *Rev. Mod. Phys.* **71**, 735 (1999).
- ²Y. I. Kolesnichenko, *At. Energ* **23**, 289 (1967).
- ³A. Mikhailovskii, *Zh. Eksp. Teor. Fiz* **68**, 25 (1975).
- ⁴M. Rosenbluth and P. Rutherford, *Phys. Rev. Lett.* **34**, 1428 (1975).
- ⁵L. Chen, *Physics of Plasmas* **1**, 1519 (1994).
- ⁶A. Fasoli, C. Gormenzano, H. Berk, B. Breizman, S. Briguglio, D. Darrow, N. Gorelenkov, W. Heidbrink, A. Jaun, S. Konovalov, R. Nazikian, J.-M. Noterdaeme, S. Sharapov, K. Shinohara, D. Testa, K. Tobita, Y. Todo, G. Vlad, and F. Zonca, *Nuclear Fusion* **47**, S264 (2007).
- ⁷L. Chen and F. Zonca, *Review of Modern Physics* **88**, 015008 (2016).
- ⁸F. Zonca, L. Chen, S. Briguglio, G. Fogaccia, A. V. Milovanov, Z. Qiu, G. Vlad, and X. Wang, *Plasma Physics and Controlled Fusion* **57**, 014024 (2015).
- ⁹R. Nazikian, G. Y. Fu, M. E. Austin, H. L. Berk, R. V. Budny, N. N. Gorelenkov, W. W. Heidbrink, C. T. Holcomb, G. J. Kramer, G. R. McKee, M. A. Makowski, W. M. Solomon, M. Shafer, E. J. Strait, and M. A. V. Zeeland, *Phys. Rev. Lett.* **101**, 185001 (2008).
- ¹⁰Z. Qiu, L. Chen, and F. Zonca, *Nuclear Fusion* **56**, 106013 (2016).
- ¹¹Z. Qiu, L. Chen, and F. Zonca, *Nuclear Fusion* **57**, 056017 (2017).
- ¹²M. Falessi, L. Chen, Z. Qiu, and F. Zonca, to be submitted to *New Journal of Physics* (2023).
- ¹³F. Zonca, L. Chen, M. Falessi, and Z. Qiu, *Journal of Physics: Conference Series* **1785**, 012005 (2021).
- ¹⁴A. Di Siena, R. Bilato, T. Görler, A. B. Navarro, E. Poli, V. Bobkov, D. Jarema, E. Fable, C. Angioni, Y. O. Kazakov, *et al.*, *Physical Review Letters* **127**, 025002 (2021).
- ¹⁵H. Han, S. Park, C. Sung, J. Kang, Y. Lee, J. Chung, T. S. Hahm, B. Kim, J.-K. Park, J. Bak, *et al.*, *Nature* **609**, 269 (2022).
- ¹⁶M. Romanelli, A. Zocco, F. Crisanti, J.-E. Contributors, *et al.*, *Plasma Physics and Controlled Fusion* **52**, 045007 (2010).
- ¹⁷G. Tardini, J. Hobirk, V. Igochine, C. Maggi, P. Martin, D. McCune, A. Peeters, A. Sips, A. Stäbler, J. Stober, and the ASDEX Upgrade Team, *Nuclear Fusion* **47**, 280 (2007).
- ¹⁸C. Bourdelle, G. Hoang, X. Litaudon, C. Roach, and T. Tala, *Nuclear fusion* **45**, 110 (2005).
- ¹⁹A. Di Siena, T. Görler, H. Doerk, E. Poli, and R. Bilato, *Nuclear Fusion* **58**, 054002 (2018).
- ²⁰N. Bonanomi, P. Mantica, A. D. Siena, E. Delabie, C. Giroud, T. Johnson, E. Lerche, S. Menmuir, M. Tsalas, D. V. Eester, and J. Contributors, *Nuclear Fusion* **58**, 056025 (2018).
- ²¹J. Citrin, J. Garcia, T. Görler, F. Jenko, P. Mantica, D. Told, C. Bourdelle, D. Hatch, G. Hogewej, T. Johnson, *et al.*, *Plasma Physics and Controlled Fusion* **57**, 014032 (2014).
- ²²J. Citrin and P. Mantica, *Plasma Physics and Controlled Fusion* **65**, 033001 (2023).
- ²³J. Citrin, F. Jenko, P. Mantica, D. Told, C. Bourdelle, J. Garcia, J. W. Haverkort, G. M. D. Hogewej, T. Johnson, and M. J. Pueschel, *Phys. Rev. Lett.* **111**, 155001 (2013).
- ²⁴V. Marchenko, *Physics of Plasmas* **29**, 030702 (2022).
- ²⁵C. Cheng, L. Chen, and M. Chance, *Ann. Phys.* **161**, 21 (1985).
- ²⁶A. Hasegawa, C. G. MacLennan, and Y. Kodama, *Physics of Fluids* **22**, 2122 (1979).
- ²⁷M. N. Rosenbluth and F. L. Hinton, *Phys. Rev. Lett.* **80**, 724 (1998).
- ²⁸S. Mazzi, J. Garcia, D. Zarzoso, Y. O. Kazakov, J. Ongena, M. Dreval, M. Nocente, Ž. Štancar, G. Szepesi, J. Eriksson, *et al.*, *Nature Physics* **18**, 776 (2022).
- ²⁹L. Chen, Z. Qiu, and F. Zonca, *Nuclear Fusion* **62**, 094001 (2022).
- ³⁰L. Chen, Z. Qiu, and F. Zonca, *Nuclear Fusion* **63**, 106016 (2023).
- ³¹L. Chen and F. Zonca, *Phys. Rev. Lett.* **109**, 145002 (2012).
- ³²F. Zonca, L. Chen, S. Briguglio, G. Fogaccia, G. Vlad, and X. Wang, *New Journal of Physics* **17**, 013052 (2015).
- ³³L. Chen, Z. Lin, and R. White, *Physics of Plasmas* **7**, 3129 (2000).
- ³⁴Z. Lin, T. S. Hahm, W. W. Lee, W. M. Tang, and R. B. White, *Science* **281**, 1835 (1998).
- ³⁵Y. Todo, H. Berk, and B. Breizman, *Nuclear Fusion* **50**, 084016 (2010).
- ³⁶A. Biancalani, A. Bottino, P. Lauber, A. Mishchenko, and F. Vannini, *Journal of Plasma Physics* **86**, 825860301 (2020).
- ³⁷Z. Qiu, L. Chen, and F. Zonca, *Physics of Plasmas* (1994-present) **23**, 090702 (2016).
- ³⁸L. Chen, Z. Qiu, F. Zonca, M. V. Falessi, P. Liu, and R. Ma, in *The 14th International West Lake Symposium-Frontier Progress in Fusion Energy Research and Development* (2023).
- ³⁹N. Chen, H. Hu, X. Zhang, S. Wei, and Z. Qiu, *Physics of Plasmas* **28**, 042505 (2021).
- ⁴⁰E. A. Frieman and L. Chen, *Physics of Fluids* **25**, 502 (1982).
- ⁴¹J. Connor, R. Hastie, and J. Taylor, *Phys. Rev. Lett.* **40**, 396 (1978).
- ⁴²H. Y. Wang, I. Holod, Z. Lin, J. Bao, J. Y. Fu, P. F. Liu, J. H. Nicolau, D. Spong, and Y. Xiao, *Physics of Plasmas* **27**, 082305 (2020).
- ⁴³G. Dong, J. Bao, A. Bhattacharjee, and Z. Lin, *Physics of Plasmas* **26** (2019).
- ⁴⁴C. Z. Cheng and L. Chen, *The Physics of Fluids* **23** (1980).
- ⁴⁵P. N. Guzdar, L. Chen, W. M. Tang, and P. H. Rutherford, *The Physics of Fluids* **26**, 673 (1983).
- ⁴⁶L. Chen, S. Briguglio, and F. Romanelli, *Physics of Fluids B: Plasma Physics* **3**, 611 (1991).

⁴⁷W. W. Heidbrink, N. N. Gorelenkov, Y. Luo, M. A. Van Zee-land, R. B. White, M. E. Austin, K. H. Burrell, G. J. Kramer,

M. A. Makowski, G. R. McKee, and R. Nazikian (the DIII-D team), *Phys. Rev. Lett.* **99**, 245002 (2007).